


Article

New Secondary Metabolites from the Marine-Derived Fungus *Talaromyces mangshanicus* BTBU20211089

Kai Zhang ^{1,†}, Xinwan Zhang ^{2,†}, Rui Lin ², Haijin Yang ², Fuhang Song ^{1,*} , Xiuli Xu ^{2,*} and Long Wang ^{3,*}

¹ School of Light Industry, Beijing Technology and Business University, Beijing 100048, China; zhangkai2030302071@st.btbu.edu.cn

² School of Ocean Sciences, China University of Geosciences, Beijing 100083, China; zhangxinwan@cugb.edu.cn (X.Z.); linrui520@126.com (R.L.); yanghaijin52@163.com (H.Y.)

³ Key Laboratory of Mycology, Institute of Microbiology, Chinese Academy of Sciences, Beijing 100101, China

* Correspondence: songfuhang@btbu.edu.cn (F.S.); xuxl@cugb.edu.cn (X.X.); wl_dgk@im.ac.cn (L.W.)

† These authors contributed equally to this work.

Abstract: Seven new compounds, namely talaromanloid A (1), talaromydene (2), 10-hydroxy-8-demethyltalaromydine and 11-hydroxy-8-demethyltalaromydine (3 and 4), talaromylectone (5), and ditalaromylectones A and B (6 and 7), together with seven known compounds were identified from a marine-derived fungus, *Talaromyces mangshanicus* BTBU20211089, which was isolated from a sediment sample collected from the South China Sea. Their chemical structures were determined using spectroscopic data, including HRESIMS, 1D, and 2D NMR techniques. The absolute configurations of 1 and 2 were elucidated by comparing experimental and calculated ECD spectra. Compounds 1, 2, 6 and 7 are new compounds possessing a novel carbon skeleton. Compound 6 is a dimeric molecule of 3 and 9. Compound 7 shared a unique structure of the cyclized dimer of 3 and 4. All the compounds were tested for their bioactivities against *Staphylococcus aureus*, *Escherichia coli*, and *Candida albicans*.

Keywords: marine-derived fungus; *Talaromyces mangshanicus*; antifungal; antibacterial



Citation: Zhang, K.; Zhang, X.; Lin, R.; Yang, H.; Song, F.; Xu, X.; Wang, L. New Secondary Metabolites from the Marine-Derived Fungus *Talaromyces mangshanicus* BTBU20211089. *Mar. Drugs* **2022**, *20*, 79. <https://doi.org/10.3390/md20020079>

Academic Editor: Ekaterina Yurchenko

Received: 24 December 2021

Accepted: 12 January 2022

Published: 18 January 2022

Publisher's Note: MDPI stays neutral with regard to jurisdictional claims in published maps and institutional affiliations.



Copyright: © 2022 by the authors. Licensee MDPI, Basel, Switzerland. This article is an open access article distributed under the terms and conditions of the Creative Commons Attribution (CC BY) license (<https://creativecommons.org/licenses/by/4.0/>).

1. Introduction

Marine-derived fungi represent the most prolific source of new chemical entries with diverse bioactivities [1,2]. *Talaromyces* species had been included in the *Penicillium* subgenus *Biverticillium* and were classified as a valid genus by McNeill [3]. The *Talaromyces* fungus, widely distributed in marine and terrestrial environments, is an important natural resource producing enzymes and pigments of industrial importance, and sometimes can cause invasive mycosis. Different classes of secondary metabolites, such as polyene and isocoumarin [4], oxaoones and oxaphenalenones [5], meroterpenoids [6], oxaphenalenone [7], diphenyl ether derivatives, and sesquiterpene-conjugated amino acids [8,9], have been characterized from marine-derived *Talaromyces* strains.

During our ongoing investigations into bioactive natural products from marine-derived microorganisms [10–13], a fungal strain of *Talaromyces mangshanicus* BTBU20211089, which was isolated from a sediment sample collected from the South China Sea, was found to be active against *Candida albicans*. Chemical investigation of this fungus cultured in rice solid media led to the isolation and identification of seven new compounds, namely, talaromanloid A (1), talaromydene (2), 10-hydroxy-8-demethyltalaromydine and 11-hydroxy-8-demethyltalaromydine (3 and 4), talaromylectone (5), and ditalaromylectones A and B (6 and 7), together with seven known compounds. The known compounds were determined to be 3-(propan-2-ylidene)-pyrrolidine-2, 5-dione (8) [14], (E)-3-(2,5-dioxo-3-(propan-2-ylidene)pyrrolidin-1-yl)acrylic acid (9) [15], nafuredin (10) [16], dehydroaustinol (11) [17], austinolide (12) [18], altenusin (13), and 5'-methoxy-6-methyl-biphenyl-3,4,3'-triol (14) [19] (Figure 1). Here, we report the isolation, structure elucidation, and bioactivities of these compounds.

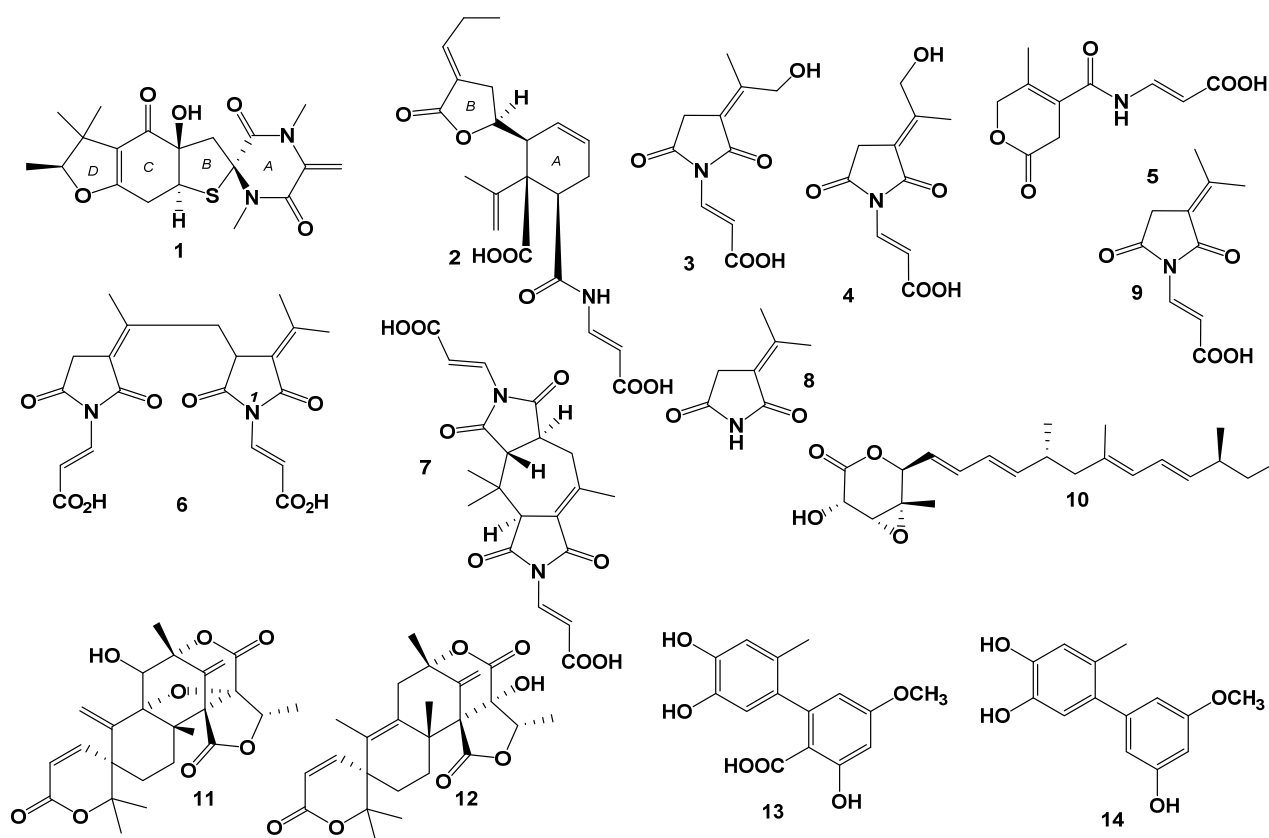


Figure 1. Chemical structures of 1–14.

2. Results

2.1. Structure Elucidation

Compound **1** was isolated as a light-yellow powder. The molecular formula of **1** was determined to be $C_{19}H_{24}N_2O_5S$ based on the HRESIMS spectrum (m/z $[M + H]^+$ 393.1481, calcd for $C_{19}H_{25}N_2O_5S$, 393.1479), accounting for nine degrees of unsaturation (Figure S1). The 1H NMR, ^{13}C , and HSQC spectra of **1** (Figures S2–S4, Table 1) demonstrated signals for one terminal double bond (δ_H 5.57 (1H, H-17a) and 5.08 (1H, H-17b)/ δ_C 136.0 (C-3) and 102.8 (C-17)), two sp^3 methylenes (δ_H 3.37 (1H, H-7a) and 2.86 (1H, H-7b)/ δ_C 42.6 (C-7), 3.02 (1H, H-15a) and 2.47 (1H, H-15b)/ δ_C 21.6 (C-15)), one sp^3 oxygenated methine (δ_H 4.42 (1H, H-12)/ δ_C 90.7 (C-12)), one sp^3 methine (δ_H 4.18 (1H, H-16)/ δ_C 50.9 (C-16)), four singlet methyl groups (δ_H 3.19 (3H, H-18)/ δ_C 30.7 (C-18), δ_H 2.83 (3H, H-19)/ δ_C 25.9 (C-19), δ_H 1.01 (3H, H-20)/ δ_C 20.2 (C-20), δ_H 1.29 (3H, H-21)/ δ_C 24.8 (C-21)), one doublet methyl (δ_H 1.28 (3H, H-22)/ δ_C 13.9 (C-22)), one ketone carbonyl at δ_C 190.8 (C-9), two amide carbonyls at δ_C 158.0 (C-1) and 165.7 (C-3), one oxygenated sp^2 quaternary carbon at δ_C 171.1 (C-14), two sp^2 quaternary carbons at δ_C 136.0 (C-2) and 116.9 (C-10), and two sp^3 quaternary carbons at δ_C 72.2 (C-5) and 81.6 (C-8). The downfield shift of oxygenated methine (C-12) in the ^{13}C spectrum was consistent with that of phomalirazine [20]. Detailed analysis of the 2D NMR data (Figures S4–S6) confirmed the structure of **1**. The HMBC correlations (Figure 2) between H-17b and C-2, H₂-17 and C-1, H₃-18 and C-2 and C-4, and H₃-19 and C-1 and C-5 revealed the *N,N*-dimethyldiketopiperazine moiety of ring A. The long-range HMBC correlations between H-15b and C-8, H₂-15 and C-10 and C-14, and H-16 and C-8, C-9, and C-14 indicated the presence of the cyclopentenone moiety of ring C. The HMBC crossing peaks from H-7a to C-16, and H₂-7 to C-4, C-5, C-8, and C-9 revealed that rings A and C were linked from C-5 to C-8 through C-7. The HMBC correlations between H₃-20 and H₃-21 and C-10, C-11, and C-12, and H₃-22 and C-11 and C-12 indicated that the 1,1-dimethylpropyl was attached to C-10 by C-11. By analyzing the downfield chemical

shifts of C-5, C-12, and C-14 and the molecular formula, C-5 and C-16 were linked by a sulfur atom to form the tetrahydrothiophene moiety of ring B, and C-12 and C-14 were linked by an oxygen atom to form the dihydrofuran moiety of ring D. Therefore, the planar structure of **1** was assigned. The absolute configurations of **1** were established as 5*S*, 8*R*, 12*S*, and 16*S* by comparing the experimental and calculated ECD spectra (Figure 3). Thus, the structure of **1** was determined and named talaromanloid A.

Table 1. ^1H (500 MHz) and ^{13}C NMR (125 MHz) data of **1** and **2** (DMSO- d_6).

Position	1		2	
	δ_{C} , Type	δ_{H} (J in Hz)	δ_{C} , Type	δ_{H} (J in Hz)
1	158.0, C		169.9, C	
2	136.0, C		44.7, CH	2.90, t (8.5)
3			25.1, CH ₂	2.34, m
4	165.7, C		129.7, CH	6.05, m
5	72.2, C		123.1, CH	5.82, dd (10.0, 1.5)
6			45.5, CH	3.20, m
7	42.6, CH ₂	3.37, d (14.5) 2.86, d (14.5)	57.9, C	5.05, s
8	81.6, C		140.8, C	
9	190.8, C		115.0, CH ₂	5.05, s 4.68, s
10	116.9, C		19.6, CH ₃	1.84, s
11	42.7, C		80.3, CH	4.47, ddd (10.0, 4.0, 4.0)
12	90.7, CH	4.42, q (7.0)	27.7, CH ₂	2.56, m
13			127.6, C	
14	171.1, C		168.5, C	
15	21.6, CH ₂	3.02, dd (19.5, 6.0) 2.47, overlap	146.7, CH	6.77, t (7.5)
16	50.9	4.18, dd (6.0, 1.0)	21.9, CH ₂	2.13, dq (7.5, 7.5)
17	102.8, CH ₂	5.57, d (1.0) 5.08, d (1.0)	13.1, CH ₃	0.98, t (7.5)
18	30.7, CH ₃	3.19, s	176.5, C	
19	29.5, CH ₃	2.83, s	137.9, CH	7.70, dd (14.0, 11.0)
20	20.2, CH ₃	1.01, s	101.6, CH	5.49, d (14.0)
21	24.8, CH ₃	1.29, s	168.5, C	
22	13.9, CH ₃	1.28, s (5.5)		
NH				10.26, d (11.0)

Compound **2** was isolated as a light-yellow powder. The molecular formula of **2** was determined to be C₂₁H₂₅NO₇ based on the HRESIMS spectrum (m/z [M + H]⁺ 404.1701, calcd for C₂₁H₂₆NO₇, 404.1704), accounting for ten degrees of unsaturation (Figure S8). The ^1H and ^{13}C NMR spectra, along with HSQC data (Figures S9–S11, Table 1), revealed the presence of two methyls (δ_{H} 1.84/ δ_{C} 19.6 (C-10); δ_{H} 0.98/ δ_{C} 13.1 (C-17)), four methylenes (δ_{H} 2.34/ δ_{C} 25.1 (C-3); δ_{H} 5.05, 4.68/ δ_{C} 115.0 (C-9); δ_{H} 2.56/ δ_{C} 27.7 (C-12); δ_{H} 2.13/ δ_{C} 21.9 (C-16)), eight methines (δ_{H} 2.90/ δ_{C} 44.7 (C-2); δ_{H} 6.05/ δ_{C} 129.7 (C-4); δ_{H} 5.82/ δ_{C} 123.1 (C-5); δ_{H} 3.20/ δ_{C} 45.5 (C-6); δ_{H} 4.47/ δ_{C} 80.3 (C-11); δ_{H} 6.77/ δ_{C} 146.7 (C-15); δ_{H} 7.70/ δ_{C} 137.9 (C-19); δ_{H} 5.49/ δ_{C} 101.6 (C-20)), two sp² quaternary carbons (δ_{C} 140.8 (C-8), 127.6 (C-13)), one two sp³ quaternary carbon (δ_{C} 57.9 (C-7)), and four carbonyls (δ_{C} 169.9 (C-1), 168.5 (C-14), δ_{C} 176.5 (C-18), δ_{C} 168.5 (C-21)). The ^1H - ^1H COSY correlations (Figure S12) between H-2 and H₂-3, H-4, H-5, H-6, H-11, and H₂-12 revealed the connections of C-2, C-3, C-4, C-5, C-6, C-11, and C-12. The ^1H - ^1H COSY crossing peaks from H-15 through H₂-16 to H₃-17 suggested a side chain of C-15/C-16/C-17. The ^1H - ^1H COSY correlations between H-NH and H-19 and H-20, along with the coupling constants (δ_{H} 10.26, d (11.0), H-NH, 7.70 (dd, J = 14.0, 11.0 Hz, H-19), 5.49 (d, J = 14.0 Hz, H-20)) demonstrated the trans-double bond attached to the amino of N/C-19/C-20. In the HMBC spectrum (Figure S13), the correlations between H-2 and C-6 and C-7, and H-5 and C-7 suggested the presence of

ring A. The HMBC correlations (Figure 2) between H₂-9 and C-7 and C-10, and between H₃-10 and C-7, C-8, and C-9 indicated the connection between C-8 and C-7. The carbonyls of C-1 and C-18 were confirmed by HMBC correlations between H-2 and C-1 and C-18, and between H-NH and C-1. The acrylic acid moiety attached to NH was characterized by HMBC correlations between H-19 and C-1 and between H-19 and H-20 and C-21. Ring B was revealed by the HMBC correlations between H-11 and C-13, and between H-12 and C-13 and C-14. The HMBC correlations between H₂-16 and C-13 and C-15, together with the crossing peak from H-15 to C-14, indicated the connection between C-13 and C-15. The ROESY correlations (Figure 4 and Figure S14) between H₃-10 (δ_{H} 1.84, s) and H-2 (δ_{H} 2.90, t, J = 8.5 Hz) and H-6 (δ_{H} 3.20, m) indicated that they were on the same side of ring A. The conformation of the double bond of C-13/C-15 was deduced by the ROESY correlations between H₂-12 and H₂-16 (Figure 2 and Figure S14). By comparing the experimental and calculated ECD spectra (Figure 3), the absolute configurations of **2** were established as 2*R*, 6*S*, 7*R*, 8*S*, and 11*S*. Thus, the structure of **2** was determined and named talaromydene.

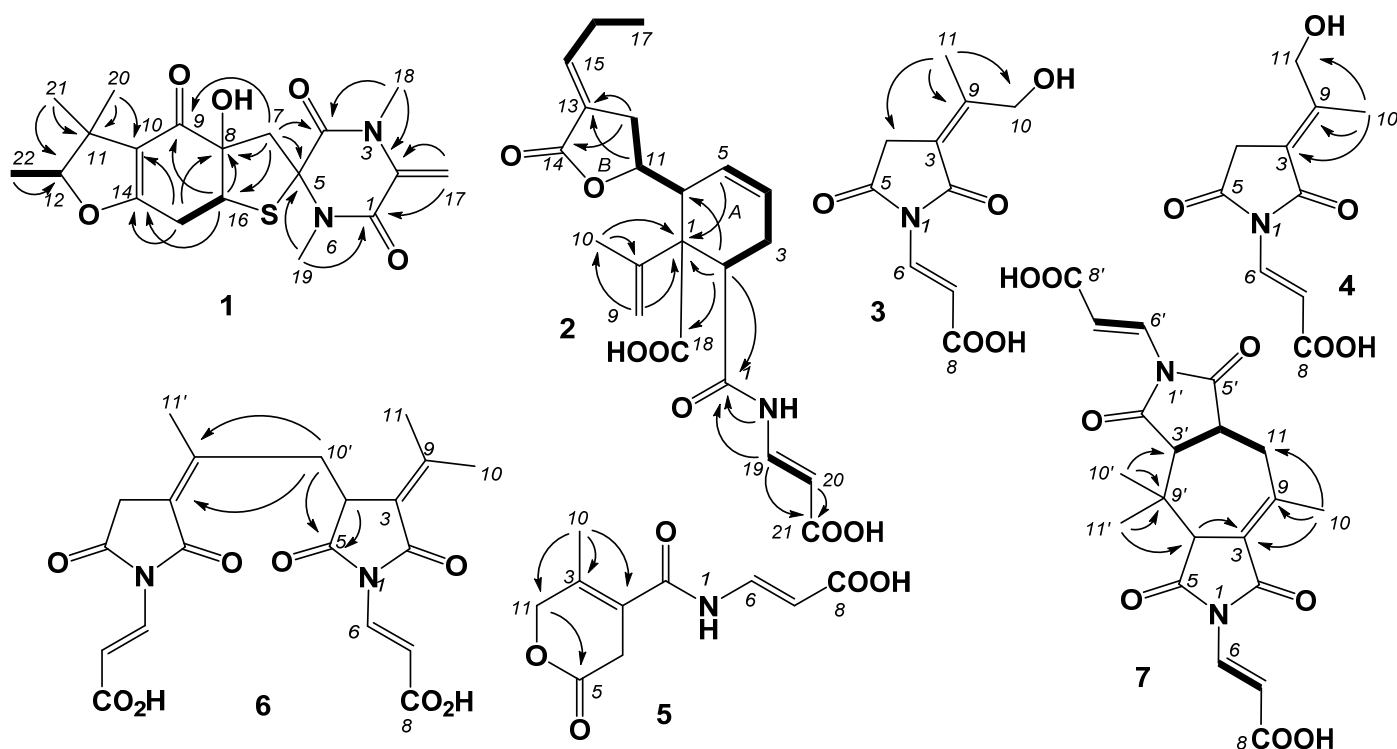


Figure 2. Key COSY (bold lines) and HMBC (arrows) correlations in 1–7.

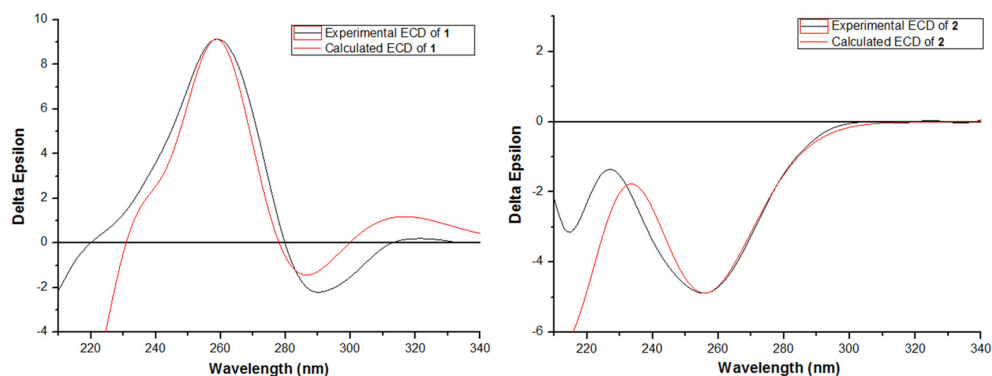


Figure 3. Calculated and experimental electronic circular dichroism (ECD) spectra of **1** and **2**.

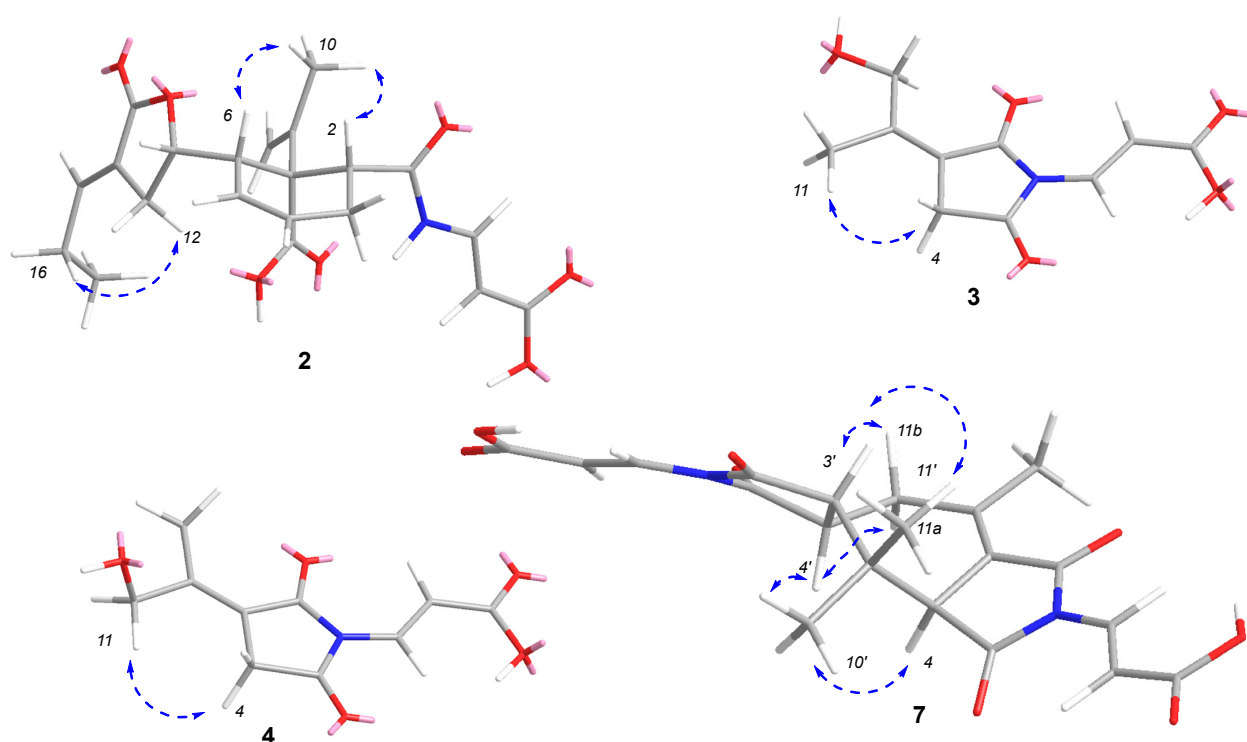


Figure 4. ROESY correlations in 2–4 and 7.

Compound **3** was isolated as a colorless powder. The molecular formula of **3** was determined to be $C_{10}H_{11}NO_5$ based on the HRESIMS spectrum (m/z $[M + H]^+$ 226.0716, calcd for $C_{10}H_{12}NO_5$, 226.0710), accounting for six degrees of unsaturation (Figure S15). The 1H and ^{13}C NMR spectra, along with HSQC data (Figures S16–S18, Table 2), revealed the presence of one trans-double bond (δ_H 7.55 (d, $J = 14.5$ Hz)/ δ_C 131.3 (C-6); 6.73 (d, $J = 14.5$ Hz)/ δ_C 109.2 (C-7)), one sp^3 methylene (δ_H 3.40/ δ_C 33.6 (C-4)), one sp^3 oxygenated methylene (δ_H 4.66/ δ_C 60.0 (C-10)), one methyl group (δ_H 1.91/ δ_C 18.1 (C-11)), two sp^2 quaternary carbons (δ_C 117.8 (C-3); 156.2 (C-9)), and three carbonyls (δ_C 166.5 (C-2), 172.5 (C-5), 167.8 (C-8)). The NMR data were similar to those of (*E*)-3-(2,5-dioxo-3-(propan-2-ylidene)pyrrolidin-1-yl)acrylic acid [15], although one of the methyl groups was replaced by a hydroxymethyl in **3**. The hydroxyl of C-10 was confirmed by the HMBC correlations (Figure 2 and Figure S19) between H_3 -11 and C-3, C-9, and C-10, and ROESY correlation (Figure 4 and Figure S20) between H_3 -11 and H_2 -4. Thus, the structure of **3** was determined and named 10-hydroxy-8-demethyltalaromydine.

Compound **4** was isolated as a colorless powder. The molecular formula of **4** was determined to be $C_{10}H_{11}NO_5$ based on the HRESIMS spectrum (m/z $[M + H]^+$ 226.0716, calcd for $C_{10}H_{12}NO_5$, 226.0710), accounting for six degrees of unsaturation (Figure S21). The 1H , ^{13}C NMR, and HSQC data (Figures S22–S24, Table 2) shared high similarity with those of **3**. The hydroxyl of C-11 was confirmed by the HMBC correlations (Figure 2 and Figure S25) between H_3 -10 and C-3, C-9, and C-11, and ROESY correlation (Figure 4 and Figure S26) between H_2 -11 and H_2 -4. Thus, the structure of **4** was determined and named 11-hydroxy-8-demethyltalaromydine.

Compound **5** was isolated as a colorless powder. The molecular formula of **5** was determined to be $C_{10}H_{11}NO_5$ based on the HRESIMS spectrum (m/z $[M + H]^+$ 226.0715, calcd for $C_{10}H_{12}NO_5$, 226.0710), accounting for six degrees of unsaturation (Figure S27). The 1H , ^{13}C , NMR, and HSQC data (Figures S28–S30, Table 2) shared high similarity with those of **3** and **4**. The signal at δ_H 10.59 (brs, H-NH) in the 1H spectrum and 1H - 1H COSY correlation between H-NH and H-6 (δ_H 7.55 (br d, $J = 8.5$ Hz)) suggested that the pyrrolidine-2,5-dione in **5** was replaced by a ring-opening moiety. The HMBC correlations

(Figure 2 and Figure S32) between H₂-11 and C-5 (δ_C 168.6) revealed that C-5 and C-11 formed a lactone unit. Thus, the structure of **5** was determined and named talaromylectone.

Table 2. ¹H (500 MHz) and ¹³C NMR (125 MHz) data of **3–5** (DMSO-*d*₆).

Position	3		4		5	
	δ_C , Type	δ_H , (J in Hz)	δ_C , Type	δ_H , (J in Hz)	δ_C , Type	δ_H , (J in Hz)
2	166.5, C		167.4, C		164.7, C	
3	117.8, C		117.2, C		121.9, C	
4	33.6, CH ₂	3.40, br s	32.9, CH ₂	3.41, br d, 1.0	30.7, CH ₂	3.29, br q (2.0)
5	172.5, C		172.5, C		168.6, C	
6	131.3, CH	7.55, d (14.5)	131.3, CH	7.57, d (15.0)	137.8, CH	7.81, br d (8.5)
7	109.2, CH	6.73, d (14.5)	109.0, CH	6.74, d (15.0)	102.3, CH	5.56, d (14.0)
8	167.8, C		167.8, C		168.2, C	
9	156.2, C		154.3, C		136.6, C	
10	60.0, CH ₂	4.66, s	15.5, CH ₃	2.27, s	16.0, CH ₃	1.88, s
11	18.1, CH ₃	1.91, s	63.4, CH ₂	4.05, s	71.2, CH ₂	4.83, br s
NH						10.59, br s

Compound **6** was isolated as a light-yellow powder. The molecular formula of **6** was determined to be C₂₀H₂₀N₂O₈ based on the HRESIMS spectrum (*m/z* [M + H]⁺ 417.1287, calcd for C₂₀H₂₁N₂O₈, 417.1292), accounting for twelve degrees of unsaturation (Figure S33). The ¹H and ¹³C NMR spectra, along with the HSQC data (Figures S34–S36, Table 3), revealed that **6** is a dimeric analog of **3** and (*E*)-3-(2,5-dioxo-3-(propan-2-ylidene)pyrrolidin-1-yl)acrylic acid (**9**). The proton NMR spectrum showed signals for three singlet methyl groups at δ_H 2.30 (H₃-10), 2.03 (H₃-11), and 1.95 (H₃-11'), one singlet methylene at δ_H 3.46 (H₂-4'), and one coupled methylene at δ_H 3.31 (dd, *J* = 13.0, 10.0 Hz, H-10'a) and 3.01 (dd, *J* = 13.0, 6.5 Hz, H-10'b) with one methine at δ_H 3.83 (dd, *J* = 10.0, 6.5 Hz, H-4), which revealed that one of the methyl groups in the monomer was replaced by methylene and attached to the methine of the other monomer. The linkage of C-4 and C-10' was confirmed by the HMBC correlations (Figure 2 and Figure S37) between H₂-10' and C-3' (δ_C 121.2) and C-9' (δ_C 150.5), and between H₂-10' and H-4 and C-5 (δ_C 173.7). Therefore, the structure of **6** was determined and named ditalaromylectone A.

Table 3. ¹H (500 MHz) and ¹³C NMR (125 MHz) data of **6** and **7** (DMSO-*d*₆).

Position	6		7	
	δ_C , Type	δ_H , mult (J in Hz)	δ_C , Type	δ_H , mult (J in Hz)
2	166.8, C		166.5, C	
3	122.1, C		119.0, C	
4	42.1, CH	3.83, dd (10.0, 6.5)	49.9, CH	3.70, s
5	173.7, C		173.3, C	
6	131.0, CH	7.53, d (15.0)	130.7, CH	7.57, d (15.0)
7	109.6, CH	6.70, d (15.0)	110.0, CH	6.77, d (15.0)
8	167.7, C		167.5, C	
9	153.7, C		155.6, C	
10	21.1, CH ₃	2.30, s	21.2, CH ₃	2.31, s
11	23.8, CH ₃	2.03, s	37.8, CH ₂	3.07, dd (19.5, 7.5) 2.71, dd (19.5, 11.0)
2'	166.3, C		174.5, C	
3'	121.2, C		52.0, CH	2.90, d (8.5)
4'	33.8, CH ₂	3.46, s	36.7, CH	3.62, m
5'	172.0, C		175.9, C	
6'	131.0, CH	7.51, d (15.0)	130.7, CH	7.46, d (15.0)
7'	109.6, CH	6.61, d (15.0)	109.8, CH	6.70, d (15.0)
8'	166.7, C		167.5, C	
9'	150.5, C		39.1, C	
10'	35.4, CH ₂	3.31, dd (13.0, 10.0) 3.01, dd (13.0, 6.5)	20.4, CH ₃	1.31, s
11'	22.5, CH ₃	1.95, s	22.1, CH ₃	1.06, s

Compound **7** was isolated as a light-yellow powder. The molecular formula of **7** was determined to be $C_{20}H_{20}N_2O_8$ based on the HRESIMS spectrum (m/z $[M + H]^+$ 417.1289, calcd for $C_{20}H_{21}N_2O_8$, 417.1292), accounting for twelve degrees of unsaturation (Figure S38). The 1H and ^{13}C NMR spectra, along with the HSQC data (Figures S39–S41, Table 3), revealed that **7** is a dimeric analog of **4**, which possessed a different skeleton to that of **6**. The 1H - 1H COSY correlations (Figure S42) between H_2 -11 and H -4', and between H -3' and H -4', indicated the connection of C -11/ C -4'/ C -3'. The HMBC correlations (Figure 2 and Figure S43) between H -4 and C -3, H_3 -10 and C -3, C -9, and C -11, and H_3 -10' and H_3 -11' and C -4, C -3', and C -9' confirmed the presence of the cycloheptene moiety. In the ROESY spectra (Figure S44), the correlations between H -3' (δ_H 2.90) and H -11b (δ_H 2.71)/ H_3 -11' (δ_H 1.06), between H -4' (δ_H 3.62) and H -11a (δ_H 3.07)/ H_3 -10' (δ_H 1.31), and between H -4 (δ_H 3.70) and H_3 -10' suggested the relative configurations of **7**. The optical rotation is near zero, so **7** was assigned as a racemic mixture and named ditalaromylectone B.

Seven known compounds, including 3-(propan-2-ylidene)pyrrolidine-2, 5-dione (**8**), (E)-3-(2,5-dioxo-3-(propan-2-ylidene)pyrrolidin-1-yl)acrylic acid (**9**), nafuredin (**10**), dehydroaustinol (**11**), austinolide (**12**), altenusin (**13**), and 5'-methoxy-6-methyl-biphenyl-3,4,3'-triol (**14**), were identified by comparing the NMR data with the corresponding reported data.

The biosynthesis of **2–9** most likely proceeds via the same precursors, and plausible biosynthetic relationships of **3–5** and **7–9** are presented in Figure 5. Precursors **15** and **16** may be derived from the tricarboxylic acid cycle [21] and then form **9** by an amidation reaction. Compound **8** is produced by the oxidation of **9**. Compound **5** is proposed to be generated after the oxidation, cyclization, and amidation of **15** or **16**. Compound **7** is proposed to be derived from the cyclization of **9** and dehydration of **4**.

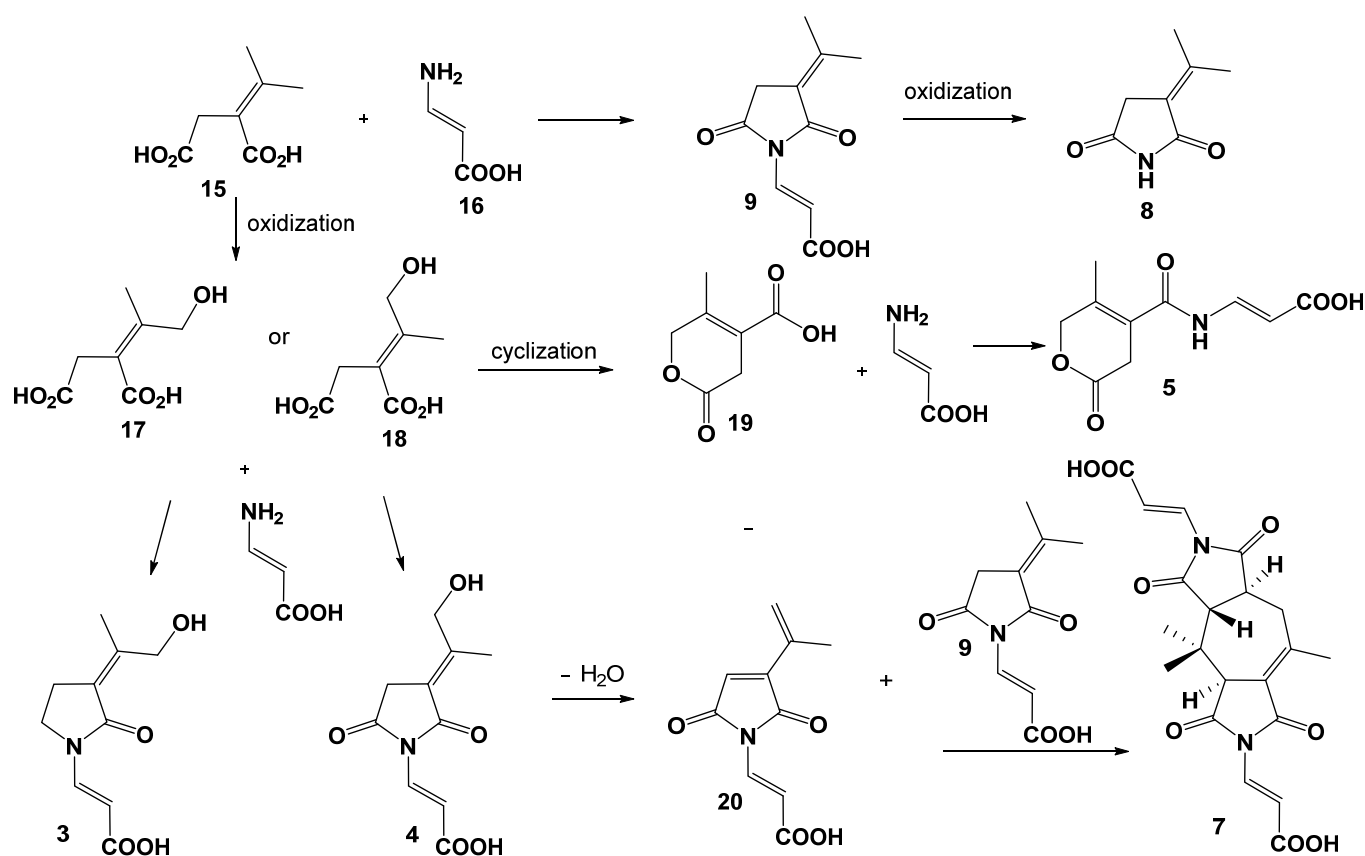


Figure 5. Plausible biosynthetic relationships of **3–5** and **7–9**.

2.2. Biological Activity

These compounds were evaluated for their antibacterial activities against *Candida albicans* ATCC 10231, *Staphylococcus aureus* ATCC 25923, and *Escherichia coli* ATCC 25923. Compounds **6** and **13** showed an inhibitory effect against *C. albicans* with an MIC value of 200 µg/mL. Compounds **13** and **14** exhibited antibacterial activity against *S. aureus* with MIC values of 50 µg/mL.

3. Materials and Methods

3.1. General Experimental Procedures

Optical rotations ($[\alpha]_D^{25}$) were measured on an Anton Paar MCP 200 Modular Circular Polarimeter (Austria) in a 100 × 2 mm cell. CD spectra were recorded on an Applied Photophysics Chirascan spectropolarimeter (Surrey, UK). NMR spectra were obtained on a Bruker Avance 500 spectrometer with residual solvent peaks as references (DMSO- d_6 : δ_H 2.50, δ_C 39.52). High-resolution ESIMS measurements were obtained on an Accurate-Mass-Q-TOF LC/MS 6520 instrument (Santa Clara, CA, USA) in the positive ion mode. HPLC was performed using an Agilent 1200 Series separation module equipped with an Agilent 1200 Series diode array, Agilent 1260 Series fraction collector, and Agilent ZORBAX SB-C18 column (250 × 9.4 mm, 5 µm).

3.2. Microbial Material, Fermentation, Extraction and Purification

Strain *Talaromyces mangshanicus* BTBU20211089 was isolated from a mud sample collected from a sediment sample collected from the South China Sea and grown on a potato dextrose agar plate at 28 °C. The genomic DNA of BTBU20211089 was extracted using a Fungi Genomic DNA Extraction Kit (Solarbio Life Sciences, Beijing, China). The ITS region was amplified by using a conventional primer pair of ITS4 (5' -TCCTCCGCTTATTGATATGC -3') and ITS5 (5' -GGAAGTAAAAGTCGTAACAAGG -3'). PCR products were sent to Beijing Qingke Biotechnology Co., Ltd. (Beijing, China) for DNA sequencing and deposited in GenBank (accession number, OL905958). BTBU20211089 was identified as *Talaromyces mangshanicus* by comparing the internal transcribed spacer (ITS) region sequence with the GenBank database using the BLAST program. A neighbor-joining (NJ) tree (Figure S45) was constructed using the software package Mega version 5 [22]. The fungus was assigned the accession number BTBU20211089 in the culture collection at Beijing Technology and Business University, Beijing. The strain BTBU20211089 was inoculated on a potato dextrose agar plate and cultured for 7 days. Then, a slit of agar with the fungus was cut from the plate and inoculated in ten 1 L conical flasks, each containing a solid medium consisting of rice (200 g in 200 mL distilled water), and the flasks were incubated under static conditions at 28 °C for 30 days. The cultures were extracted three times with a mixture of EtOAc:MeOH (80:20), and the combined extracts were evaporated to dryness in vacuo. The residue was suspended in distilled water and partitioned with EtOAc. Then, the EtOAc layer was dried in vacuo to yield a dark residue (14.3 g). The EtOAc fraction was fractionated by vacuum liquid silica gel chromatography (80 × 80 mm column, Silica gel 60 H for thin-layer chromatography) using a stepwise gradient of hexane/CH₂Cl₂ (4:1, 7:3, 1:1, 1:4, 1:9, 3:97, and 0:100, *v/v*) and then a stepwise gradient of MeOH/CH₂Cl₂ (1:99, 2:98, 3:97, 5:95, 5:45, 1:4, and 100:0 *v/v*) to afford 14 fractions. Fraction G was purified by HPLC (Agilent ZORBAX SB-C18, 250 × 9.4 mm, 5 µm column, 3.0 mL/min, elution with 60% to 100% acetonitrile/H₂O in 15 min) to yield **10** (5.8 mg). Fraction I was fractionated on a Sephadex LH-20 column using an isocratic elution of CH₂Cl₂:MeOH (2:1) to yield seven subfractions (I1–I7), and subfraction I2 was further purified by HPLC (Agilent ZORBAX SB-C18, 250 × 9.4 mm, 5 µm column, 3.0 mL/min, elution with 30% to 55% acetonitrile/H₂O (0–20 min), and then to 80% acetonitrile/H₂O (20–25 min)) to yield **1** (2.0 mg), **11** (10.4 mg), and **12** (14.3 mg). Subfraction I4 was further fractionated by HPLC (Agilent ZORBAX SB-C18, 250 × 9.4 mm, 5 µm column, 3.0 mL/min, elution with 30% to 100% acetonitrile/H₂O) in 15 min to **8** (R_t 5.7 min, 3.6 mg) and **9** (20.5 mg). Fraction K was fractionated on a Sephadex LH-20 column using an isocratic elution of CH₂Cl₂:MeOH (2:1) to yield eight subfractions

(K1–K8). Subfraction K3 was further fractionated by HPLC (Agilent ZORBAX SB-C18, 250 × 9.4 mm, 5 µm column, 3.0 mL/min, with 30% to 55% acetonitrile/H₂O) in 15 min to yield **2** (*R*_t 13.4 min, 3.5 mg). Subfraction K4 was further fractionated by HPLC (Agilent ZORBAX SB-C18, 250 × 9.4 mm, 5 µm column, 3.0 mL/min, elution with 30% to 100% acetonitrile/H₂O) in 15 min to yield **6** (1.7 mg). Subfraction K5 was further fractionated by HPLC (Agilent ZORBAX SB-C18, 250 × 9.4 mm, 5 µm column, 3.0 mL/min, elution with 30% acetonitrile/H₂O) in 15 min to yield **7** (1.8 mg). Subfraction K6 was further fractionated by HPLC (Agilent ZORBAX SB-C18, 250 × 9.4 mm, 5 µm column, 3.0 mL/min, elution with 10% to 27% acetonitrile/H₂O) in 15 min to yield **3** (1.8 mg), **4** (1.2 mg), and **5** (3.3 mg). Subfraction K8 was further fractionated by HPLC (Agilent ZORBAX SB-C18, 250 × 9.4 mm, 5 µm column, 3.0 mL/min, elution with 40% to 50% acetonitrile/H₂O) in 15 min to yield **13** (6.8 mg) and **14** (5.6 mg).

Talaromanloid A (**1**): Light-yellow powder; $[\alpha]_D^{25} + 43.0$ (*c* 0.1, MeOH); CD (*c* 5.0 × 10^{−5}, CH₃OH), $\lambda_{\max}(\Delta\epsilon)$ 259 nm (+9.14) and 290 nm (−2.20); ¹H and ¹³C NMR data, Table 1; HRESIMS *m/z* 393.1481 [M + H]⁺ (calcd for C₁₉H₂₅N₂O₅S, 393.1479).

Talaromydene (**2**): Light-yellow powder; $[\alpha]_D^{25} - 67.0$ (*c* 0.1, MeOH); CD (*c* 5.0 × 10^{−5}, CH₃OH), $\lambda_{\max}(\Delta\epsilon)$ 256 nm (−4.88); ¹H and ¹³C NMR data, Table 1; HRESIMS *m/z* 404.1701 [M + H]⁺ (calcd for C₂₁H₂₆NO₇, 404.1704).

10-Hydroxydemethyltalaromydine (**3**): Colorless powder; ¹H and ¹³C NMR data, Table 2; HRESIMS *m/z* 226.0716 [M + H]⁺ (calcd for C₁₀H₁₂NO₅, 226.0710).

11-hydroxydemethyltalaromydine (**4**): Colorless powder; ¹H and ¹³C NMR data, Table 2; HRESIMS *m/z* 226.0716 [M + H]⁺ (calcd for C₁₀H₁₂NO₅, 226.0710).

Talaromylectone (**5**): Colorless powder; ¹H and ¹³C NMR data, Table 2; HRESIMS *m/z* 226.0715 [M + H]⁺ (calcd for C₁₀H₁₂NO₅, 226.0710).

Ditalaromylectone A (**6**): Light-yellow powder; $[\alpha]_D^{25} + 6.0$ (*c* 0.1, MeOH); ¹H and ¹³C NMR data, Table 3; HRESIMS *m/z* 417.1287 [M + H]⁺ (calcd for C₂₀H₂₁N₂O₈, 417.1292).

Ditalaromylectone B (**7**): Light-yellow powder; $[\alpha]_D^{25} 0.0$ (*c* 0.1, MeOH); ¹H and ¹³C NMR data, Table 3; HRESIMS *m/z* 417.1289 [M + H]⁺ (calcd for C₂₀H₂₁N₂O₈, 417.1292).

3.3. ECD Computation Method

Conformation searching was performed using OpenBabel by a genetic algorithm (GA) with the default settings [23]. The conformers were subsequently optimized using the DFT method at the B3LYP/TZVP level with GAUSSIAN 09 [24]. The TDDFT calculations of their low-energy conformations within 0–2.5 kcal/mol were performed at the same level with 40 single excited states. The solvent effect was taken into account by using the polarizable continuum model (PCM).

3.4. Biological Activity

Compounds **1–14** were evaluated for their antimicrobial activities in 96 well plates according to the Antimicrobial Susceptibility Testing Standards outlined by the Clinical and Laboratory Standards Institute document M07-A7 (CLSI) and our previous report [13]. The MIC was defined as the minimum concentration of the compound that prevented visible growth of the microbes.

4. Conclusions

Seven new compounds, talaromanloid A (**1**), talaromydene (**2**), 10-hydroxy-8-demethyltalaromydine and 11-hydroxy-8-demethyltalaromydine (**3** and **4**), talaromylectone (**5**), and ditalaromylectones A and B (**6** and **7**), and seven known compounds (**8–14**) were isolated from the marine-derived fungus *Talaromyces mangshanicus* BTBU20211089. The structures of the new compounds were elucidated by detailed spectroscopic analysis. The absolute configurations of **1** and **2** were elucidated by comparing experimental and calculated ECD spectra. Compound **6** was a dimeric molecule of **3** and **9** possessing a novel carbon skeleton.

Compound 7 possessed a unique novel carbon skeleton structure of a cyclized dimer of 3 and 4. Compounds 6 and 13 showed an inhibitory effect against *C. albicans* with an MIC value of 200 µg/mL. Compounds 13 and 14 exhibited antibacterial activity against *S. aureus* with MIC values of 50 µg/mL.

Supplementary Materials: The following supporting information can be downloaded at <https://www.mdpi.com/article/10.3390/md20020079/s1>: Figures S1–S44: HRESIMS, 1D and 2D NMR for compounds 1–7; Figure S45: Neighbor-joining phylogenetic tree of strain BTBU20211089.

Author Contributions: Data curation, K.Z., X.Z. and H.Y.; Funding acquisition, F.S., X.X. and L.W.; Investigation, K.Z., X.Z., R.L. and H.Y.; Supervision, F.S. and X.X.; Writing—original draft, X.X.; Writing—review and editing, F.S., X.X. and L.W. All authors have read and agreed to the published version of the manuscript.

Funding: This work was funded by grants from the National Key R&D Program of China (2018YFC0311000), the Key Lab of Marine Bioactive Substance and Modern Analytical Technique, SOA (MBSMAT-2019-06), the National Natural Science Foundation of China (81973204), and Research Foundation for Advanced Talents of Beijing Technology and Business University (No. 19008021176).

Institutional Review Board Statement: Not applicable.

Informed Consent Statement: Not applicable.

Data Availability Statement: Not applicable.

Conflicts of Interest: The authors declare no conflict of interest.

References

1. Carroll, A.R.; Copp, B.R.; Davis, R.A.; Keyzers, R.A.; Prinsep, M.R. Marine natural products. *Nat. Prod. Rep.* **2020**, *37*, 175–223. [[CrossRef](#)] [[PubMed](#)]
2. Carroll, A.R.; Copp, B.R.; Davis, R.A.; Keyzers, R.A.; Prinsep, M.R. Marine natural products. *Nat. Prod. Rep.* **2021**, *38*, 362–413. [[CrossRef](#)] [[PubMed](#)]
3. McNeill, J.B.F.; Buck, W.R.; Demoulin, V.; Greuter, W.; Hawksworth, D.L.H.P.; Knapp, S.; Marhold, K.; Prado, J.; Smith, G.F.; Wiersem, J.H. *International Code of Nomenclature for Algae, Fungi, and Plants (Melbourne Code)*; Regnum Vegetabile 154; Koeltz Scientific Books: Koenigstein, Germany, 2012.
4. Ma, M.Z.; Yi, W.W.; Qin, L.; Lian, X.Y.; Zhang, Z.Z. Talaromydien A and talaroisocoumarin A, new metabolites from the marine-sourced fungus *Talaromyces* sp. ZZ1616. *Nat. Prod. Res.* **2020**, *36*, 460–465. [[CrossRef](#)]
5. Liang, X.; Huang, Z.H.; Shen, W.B.; Lu, X.H.; Zhang, X.X.; Ma, X.; Qi, S.H. Talaromyxaones A and B: Unusual oxaphenalenone spirolactones as phosphatase inhibitors from the marine-derived fungus *Talaromyces purpureogenus* SCSIO 41517. *J. Org. Chem.* **2021**, *86*, 12831–12839. [[CrossRef](#)] [[PubMed](#)]
6. Huang, Z.H.; Liang, X.; Li, C.J.; Gu, Q.; Ma, X.; Qi, S.H. Talaromynoids A–I, highly oxygenated meroterpenoids from the marine-derived fungus *Talaromyces purpureogenus* SCSIO 41517 and their lipid accumulation inhibitory activities. *J. Nat. Prod.* **2021**, *84*, 2727–2737. [[CrossRef](#)]
7. Wu, B.; Ohlendorf, B.; Oesker, V.; Wiese, J.; Malien, S.; Schmaljohann, R.; Imhoff, J.F. Acetylcholinesterase inhibitors from a marine fungus *Talaromyces* sp strain LF458. *Mar. Biotechnol.* **2015**, *17*, 110–119. [[CrossRef](#)]
8. Lan, D.; Wu, B. Chemistry and bioactivities of secondary metabolites from the genus *Talaromyces*. *Chem. Biodivers* **2020**, *17*, e2000229. [[CrossRef](#)] [[PubMed](#)]
9. Nicoletti, R.; Trincone, A. Bioactive compounds produced by strains of *Penicillium* and *Talaromyces* of marine origin. *Mar. Drugs* **2016**, *14*, 37. [[CrossRef](#)]
10. Xu, X.; Han, J.; Lin, R.; Polyak, S.W.; Song, F. Two new piperazine-triones from a marine-derived *Streptomyces* sp. strain SMS636. *Mar. Drugs* **2019**, *17*, 186. [[CrossRef](#)]
11. Xu, X.; Han, J.; Wang, Y.; Lin, R.; Yang, H.; Li, J.; Wei, S.; Polyak, S.W.; Song, F. Two New Spiro-Heterocyclic gamma-Lactams from A Marine-Derived *Aspergillus fumigatus* Strain CUGBMF170049. *Mar. Drugs* **2019**, *17*, 289. [[CrossRef](#)]
12. Song, F.; Lin, R.; Yang, N.; Jia, J.; Wei, S.; Han, J.; Li, J.; Bi, H.; Xu, X. Antibacterial secondary metabolites from marine-derived fungus *Aspergillus* sp. IMCASM180035. *Antibiotics* **2021**, *10*, 377. [[CrossRef](#)] [[PubMed](#)]
13. Xu, X.; Li, J.; Zhang, K.; Wei, S.; Lin, R.; Polyak, S.W.; Yang, N.; Song, F. New isocoumarin analogues from the marine-derived fungus *Paraphoma* sp. CUGBMF180003. *Mar. Drugs* **2021**, *19*, 313. [[CrossRef](#)] [[PubMed](#)]
14. Li, J.W.; Duan, R.G.; Zou, J.H.; Chen, R.D.; Chen, X.G.; Dai, J.G. Meroterpenoids and isoberkedienolactone from endophytic fungus *Penicillium* sp. associated with *Dysoxia versipellis*. *Acta Pharm. Sin.* **2014**, *49*, 913–920.
15. Miao, F.; Yang, R.; Chen, D.D.; Wang, Y.; Qin, B.F.; Yang, X.J.; Zhou, L. Isolation, identification and antimicrobial activities of two secondary metabolites of *Talaromyces verruculosus*. *Molecules* **2012**, *17*, 14091–14098. [[CrossRef](#)]

16. Ui, H.; Shiomi, K.; Yamaguchi, Y.; Masuma, R.; Nagamitsu, T.; Takano, D.; Sunazuka, T.; Namikoshi, M.; Omura, S. Nafuredin, a novel inhibitor of NADH-fumarate reductase, produced by *Aspergillus niger* FT-0554. *J. Antibiot.* **2001**, *54*, 234–238. [[CrossRef](#)] [[PubMed](#)]
17. Xie, J.; Wu, Y.Y.; Zhang, T.Y.; Zhang, M.Y.; Peng, F.; Lin, B.; Zhang, Y.X. New antimicrobial compounds produced by endophytic *Penicillium janthinellum* isolated from *Panax notoginseng* as potential inhibitors of FtsZ. *Fitoterapia* **2018**, *131*, 35–43. [[CrossRef](#)] [[PubMed](#)]
18. Lo, H.C.; Entwistle, R.; Guo, C.J.; Ahuja, M.; Szewczyk, E.; Hung, J.H.; Chiang, Y.M.; Oakley, B.R.; Wan, C.C. Two separate Gene clusters encode the biosynthetic pathway for the meroterpenoids austinol and dehydroaustinol in *Aspergillus nidulans*. *J. Am. Chem. Soc.* **2012**, *134*, 4709–4720. [[CrossRef](#)] [[PubMed](#)]
19. Wang, Q.-X.; Bao, L.; Yang, X.-L.; Guo, H.; Yang, R.-N.; Ren, B.; Zhang, L.-X.; Dai, H.-Q.; Guo, L.-D.; Liu, H.-W. Polyketides with antimicrobial activity from the solid culture of an endolichenic fungus *Ulocladium* sp. *Fitoterapia* **2012**, *83*, 209–214. [[CrossRef](#)] [[PubMed](#)]
20. Soledade, M.; Pedras, C.; Abrams, S.R. Phomalirazine, a novel toxin from the phytopathogenic fungus *Phoma lingam*. *J. Am. Chem. Soc.* **1989**, *1*, 1904–1905.
21. Riko, R.; Nakamura, H.; Shindo, K. Studies on pyranonigrins— isolation of pyranonigrin E and biosynthetic studies on pyranonigrin A. *J. Antibiot.* **2014**, *67*, 179–181. [[CrossRef](#)] [[PubMed](#)]
22. Tamura, K.; Peterson, D.; Peterson, N.; Stecher, G.; Nei, M.; Kumar, S. MEGA5: Molecular evolutionary genetics analysis using maximum likelihood, evolutionary distance, and maximum parsimony methods. *Mol. Biol. Evol.* **2011**, *28*, 2731–2739. [[CrossRef](#)] [[PubMed](#)]
23. O’Boyle, N.M.; Banck, M.; James, C.A.; Morley, C.; Vandermeersch, T.; Hutchison, G.R. Open Babel: An open chemical toolbox. *J. Cheminform.* **2011**, *3*, 33.
24. Frisch, M.J.; Trucks, G.W.; Schlegel, H.B.; Scuseria, G.E.; Robb, M.A.; Cheeseman, J.R.; Scalmani, G.; Barone, V.; Mennucci, B.; Petersson, G.A.; et al. *Gaussian 09, Revision E.01*; Gaussian, Inc.: Wallingford, CT, USA, 2009.